Plasmids, Adenovirus, and Lentivirus—The mouse Hivep3 expression plasmid, pEF-Shn3, was a kind gift from Dr. Laurie Glimcher (Harvard Medical School). The human HIVEP3 expression plasmid pFN21A-HIVEP3 was obtained from Kazusa DNA Research Institute. The mouse type II Runx2 expression plasmid was a kind gift from Dr. Toshihisa Komori (Nagasaki University). The FLAG-Runx2-def expression plasmid has been described in our previous study (20). Mouse *Alg2* or *Runx2* cDNA was cloned from ST-2 cells by using a RT-PCR-based technique, subcloned into the entry vector, pENTR, and further transferred into the C-terminally V5-tagged expression vector, pEF-DEST51 (Invitrogen). For overexpression assays, cells were transfected with expression vectors using FuGENE 6 (Roche Applied Science) or Lipofectamine 2000 (Invitrogen). Cells transiently expressing the transgenes were selected and enriched by incubation with G418 disulfate (Nacalai Tesque) at a concentration of 250 μg/ml for 3–7 days. To generate adenovirus-carrying *Alg2* cDNA, the *Alg2* gene in the pENTR-Alg2 vector was transferred into the C-terminally V5-tagged adenovirus expression vector pAd/CMV/V5-DEST by LR recombination (Invitrogen) and was further transfected into the adenovirus-producing cell line 293A according to the manufacturer's protocol. The pAd/CMV/V5-GW/lacZ adenovirus expression vector was used to generate a control adenovirus. For generation of lentivirus carrying the *Alg2* gene, pENTR-Alg2 and pENTR-5′EF1αP were subjected to LR recombination with pLenti6.4/R4R2/V5-DEST (Invitrogen) to generate a lentiviral vector expressing C-terminally V5-tagged Alg2 from the EF1α promoter. The lentiviral expression vector or pLenti6/V5/GW-lacZ control vector was transfected into 293FT cells to generate the lentivirus. Virus infection into ST-2 cells was performed at a multiplicity of infection of 100. Cells infected with the lentivirus were selected by treatment with blasticidin S HCl (Invitrogen) at a concentration of 2.5 μg/ml. These experiments were approved by the Kagoshima University safety control committee for gene recombination techniques (number 22053).

Embryonic Bone Organ Culture—Calvarial bone and metatarsal bone (cartilage) rudiments were harvested from C57BL/6J mouse embryos at 17.5 days post-coitum (E17.5) and cultured in minimum essential medium α or DMEM/Ham's F-12 (1:1), respectively, supplemented with 10% FBS, 100 units/ml penicillin G, and 100 μg/ml streptomycin, as described (21). The bone rudiments were incubated in virus solution overnight for infection of adenovirus or lentivirus. Cultured bones and cartilages were fixed in 96% ethanol and stained with 0.015% Alcian blue 8GX in a mixture solution of 96% ethanol/acetic acid (4:1) for 1 day, followed by a dehydration step in 100% ethanol. Dehydrated bones were immersed briefly in 1% potassium hydroxide (KOH), followed by staining in 0.001% alizarin red S (Sigma) in 1% KOH for 1 day. Images were captured with stereomicroscope M165FC (Leica). The animal experiments were approved by the Institutional Animal Care and Use Committee of Kagoshima University (number MD12137).

Immunoprecipitation and Immunoblotting—For immunoprecipitation assays, COS-7 cells were transfected with Alg2-V5 and/or FLAG-Runx2 plasmids and were lysed in M-PER lysis buffer (Thermo Scientific) supplemented with aprotinin and phenylmethylsulfonyl fluoride (PMSF). The lysate was immunoprecipitated with anti-FLAG M2-agarose affinity gel (A2220, Sigma), and the M2 antibody-bound protein complex was eluted by incubation with 3×FLAG peptide (F4799, Sigma), according to the manufacturer's protocol. For immunoblotting assays, cells were lysed in either M-PER or NE-PER lysis buffer (Thermo Scientific) supplemented with aprotinin and PMSF or directly with 1× SDS sample buffer. SDS-PAGE, membrane transfer, and chemiluminescence were performed using a standard protocol. The blots were incubated with primary antibodies against Alg2 (1:1000; LS-C81338, Lifespan Biosciences), Runx2 (1:200; M-70, sc-10758, Santa Cruz Biotechnology), Runx2 (1:1000; 8G5, MBL), Sp7 (1:1000, ab22552, Abcam), Ibsp (1:1000, LS-C190916, Lifespan Biosciences), type II collagen (1:1000, LS-C175971, Lifespan Biosciences), Creb3l2 (1:1000, ab76856, Abcam), V5 (1:5000; R960-25, Invitrogen), FLAG (1:1000; M2, F1804, Sigma), and tubulin (1:1000; DM1A, T9026, Sigma) and with horseradish peroxidase (HRP)-conjugated anti-rabbit and anti-mouse secondary antibodies (1:10,000) (Cell Signaling). For examination of half-life of Runx2 protein, after overnight transfection with siRNA of *Hivep3*, ST-2 cells were treated with cycloheximide (Sigma) at 100 μg/ml, followed by immunoblotting using anti-Runx2 antibody. Signals were detected using the LAS 4000 mini image analyzer (Fujifilm).

Immunofluorescence—For immunofluorescence assays, cells transfected with Runx2 and/or Alg2-V5 expression plasmids were fixed with 4% paraformaldehyde in PBS for 30 min and treated with 0.2% Triton X-100. CAS block (Zymed Laboratories Inc.) was used for blocking. Cells were incubated with anti-Runx2 (1:100; 8G5, MBL), Alexa Fluor 568 rabbit anti-mouse IgG (1:1000; A11061, Invitrogen), and anti-V5-FITC (1:500; R619-25, Invitrogen) antibodies. Nuclei were stained with Hoechst dye (Invitrogen). Confocal fluorescent imaging was performed and analyzed using a laser scanning microscope system (LSM 700, Zeiss). For confirmation of the efficiency of virus infection in cultured bones, formalin-fixed mouse E17.5 embryo calvariae or metatarsal bones were embedded in paraffin blocks, which were sliced at a 4-μm thickness. The antigen was retrieved by Liberate Antibody Binding (L.A.B.) solution (Polysciences). A CAS block was used for blocking. Bone sections were incubated with anti-V5-FITC antibody. Images were captured with microscope AX80 and digital camera DP70 (Olympus).

Luciferase Assay—COS-7 cells or ST-2 cells were seeded in triplicate in 24-well plates and transiently transfected with the 6×OSE2 luciferase reporter plasmid (a kind gift from Dr. Toshihisa Komori), the mutant 6×OSE2 luciferase reporter plasmid (a kind gift from Dr. Gerard Karsenty, Columbia University Medical Center), the pGL4.75hRlucCMV *Renilla* vector (Promega), and expression vectors for Runx2, Alg2, or Hivep3. Dual-Luciferase assays were performed as described earlier (20) by using the GloMax 96 microplate luminometer (Promega).

Statistical Analysis—The data in this study have been expressed as mean ± S.D. values of three independent experiments. Statistical comparisons between the different treatments were performed using an unpaired Student's *t* test in

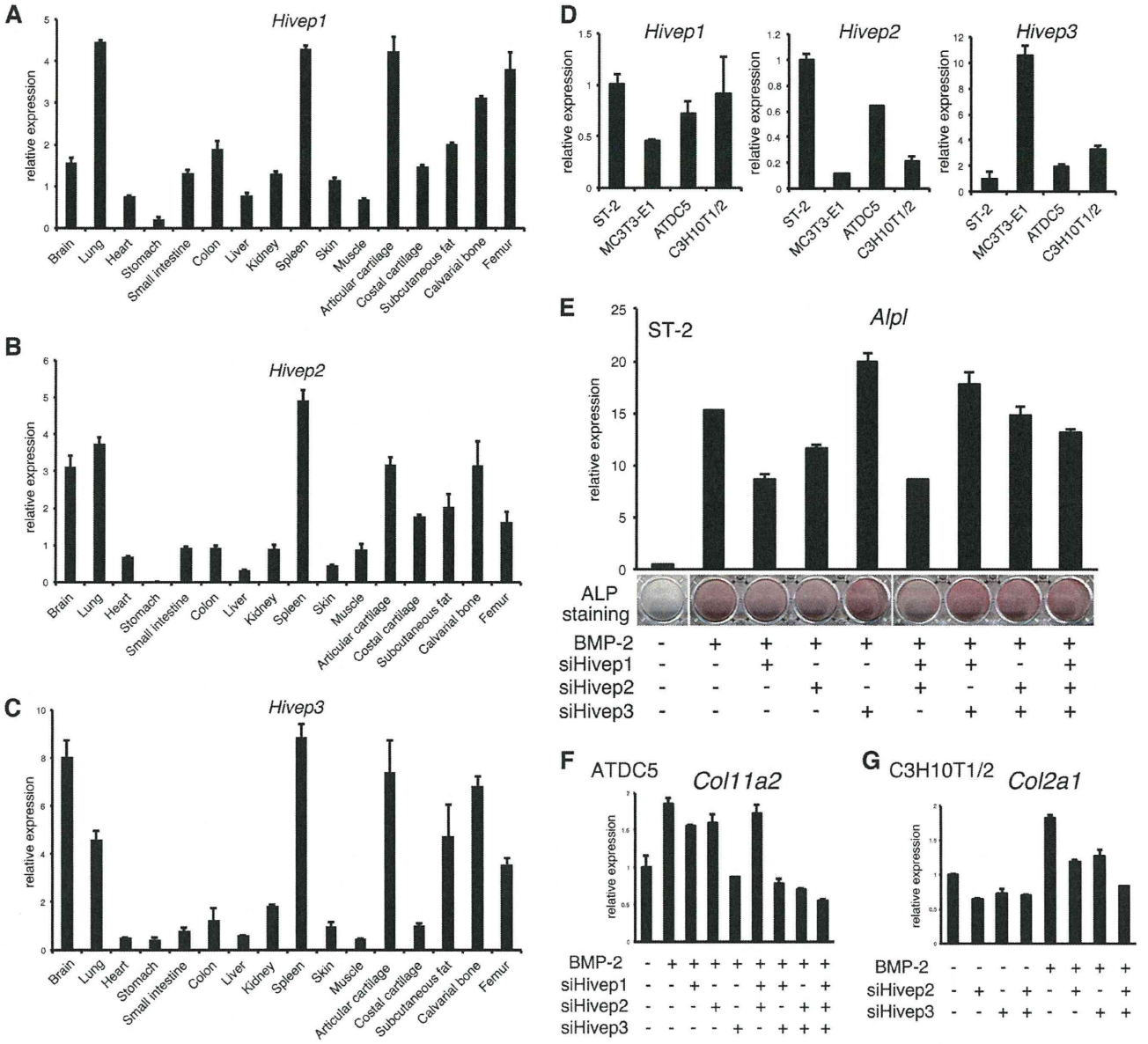

FIGURE 1. **All three Hivep genes are expressed in bone and cartilage to support osteochondrogenesis except Hivep3, which is inhibitory for osteoblast differentiation.** *A–C*, tissue cDNA panel of a 3-month-old mouse was subjected to quantitative RT-PCR (qRT-PCR) for *Hivep1* (*A*), *Hivep2* (*B*), or *Hivep3* (*C*). *D*, expression level of *Hivep1*, *Hivep2*, or *Hivep3* in the indicated cell lines was examined by qRT-PCR. *E*, ST-2 cells were transfected with siRNA for *Hivep1*, *Hivep2*, or *Hivep3* and treated with BMP-2 (300 ng/ml) for 6 days. Expression of *Alpl* was analyzed by qRT-PCR, and activity of ALP on ECM was visualized by ALP staining. *F*, ATDC5 cells were transfected with siRNA for *Hivep1*, *Hivep2*, and/or *Hivep3* and treated with BMP-2 (300 ng/ml) for 3 days. Expression of *Col11a2* was evaluated by qRT-PCR. *G*, C3H10T1/2 cells were transfected with siRNA for *Hivep2* and/or *Hivep3* and treated with BMP-2 (300 ng/ml) for 4 days. Expression of *Col2a1* was analyzed by qRT-PCR.

which $p < 0.05$ was considered significant, and $p < 0.01$ was considered highly significant.

RESULTS

Loss of Hivep1 or Hivep2 Suppresses Osteoblast Differentiation in ST-2 Cells, in Contrast to Hivep3 Silencing, and All Three Hivep siRNAs Inhibited Chondrogenesis—The precise roles of Hivep1 and Hivep2 in osteoblast differentiation are unclear. In a tissue cDNA panel from a 3-month-old adult mouse, all the Hivep genes showed a relatively specific expression pattern with high expression being observed in the lung, spleen, articular cartilage, and bone (Fig. 1, *A–C*). However, the *in vitro* results for the osteochondrogenic cell lines ST-2, MC3T3-E1, ATDC5, and C3H10T1/2 showed that the expression profiles were completely different between the Hivep genes, with *Hivep1* being expressed ubiquitously, *Hivep2* abundant in ST-2 and ATDC5, and *Hivep3* prominent in MC3T3-E1 osteoblasts (Fig. 1*D*). If the Hivep genes cooperate in osteoblast differentiation, they should regulate some common sets of genes. To test this hypothesis, ST-2 cells transfected with siRNA for *Hivep1*, *Hivep2, or Hivep3* were analyzed by a microarray assay (supplemental Tables 2–4, respectively), and the results were com-

TABLE 1

Genes down-regulated by loss of the Hivep family genes

ST-2 cells were transfected with siRNA for *Hivep1*, *Hivep2*, or *Hivep3* and treated with BMP-2 (300 ng/ml) for 2 days. mRNA samples were subjected to microarray analysis. *A*, expression of five genes was commonly decreased by all the siRNAs for the three Hivep genes. *B*, expression of six genes was commonly down-regulated by the *Hivep1* and *Hivep2* siRNAs. *C*, expression of four genes was commonly down-regulated by the *Hivep1* and *Hivep3* siRNAs. *D*, expression of three genes was commonly down-regulated by the *Hivep2* and *Hivep3* siRNAs.

A

Unique Sorted Transcript ClusterID	siCont	siHivep1	siHivep2	siHivep3	gene symbol	gene description
17305520	21.529846	11.831301	9.75173	7.9562707	*Ear1*	eosinophil-associated, ribonuclease A family, member 1
17467150	24.856544	14.449716	11.51435	15.580148	*Vmn1r18*	vomeronasal 1 receptor 18
17444697	31.70125	19.534565	21.051311	17.505947	*Cyp3a59*	cytochrome P450, subfamily 3A, polypeptide 59
17245120	44.998398	29.873207	26.863188	29.873207	*1700030O20Rik*	RIKEN cDNA 1700030O20 gene
17481207	17.905426	10.739602	10.739602	10.603919	*Olfr608*	olfactory receptor 608

B

Unique Sorted Transcript ClusterID	siCont	siHivep1	siHivep2	gene symbol	gene description
17278822	65.41499	39.391872	41.367386	*Mir679*	microRNA 679
17302598	42.895184	26.84824	22.885633	*Gm6280*	predicted gene 6280
17344852	19.322012	12.227982	11.5472975	*Olfr97*	olfactory receptor 97
17509018	24.977375	16.012548	11.412771	*Adam34*	a disintegrin and metallopeptidase domain 34
17495404	82.13324	52.76455	42.29805	*Rps13*	ribosomal protein S13
17541719	21.694231	14.250495	14.178923	*Mir450-2*	microRNA 450-2

C

Unique Sorted Transcript ClusterID	siCont	siHivep1	siHivep3	gene symbol	gene description
17356739	63.32018	36.357323	32.77719	*Mir194-2*	microRNA 194-2
17268088	22.22885	13.294091	13.626566	*Gm11543*	predicted gene 11543
17324996	19.940779	12.472511	12.472511	*Mir1947*	microRNA 1947
17516159	30.844234	20.207043	19.56977	*Olfr251|Olfr900*	olfactory receptor 251 I olfactory receptor 900

D

Unique Sorted Transcript ClusterID	siCont	siHivep2	siHivep3	gene symbol	gene description
17395379	248.2335	129.81422	142.53452	*LOC100504873*	zinc finger protein 14-like
17320035	82.69005	51.436905	49.273067	*Mir1249*	microRNA 1249
17366886	162.14816	104.84351	90.903786	*Mir467e*	microRNA 467e

pared. The expression of five genes decreased in all three knockdown experiments (Table 1, *A*), whereas six genes, four genes, or three genes were down-regulated in common by siHivep1 and siHivep2 (Table 1, *B*), siHivep1 and siHivep3 (Table 1, *C*), or siHivep2 and siHivep3 (Table 1, *D*), respectively, although no trend was observed in the purified genes. Moreover, none of the purified genes was reported to correlate with differentiation of osteoblasts or chondrocytes. To investigate the roles and possible synergism of the Hivep genes in osteoblast differentiation, the expression of the three Hivep genes was knocked down in ST-2 cells, alone or in combination (Fig. 1*E*). Although combined genetic ablation of the *Hivep2* and *Hivep3* genes in mice resulted in synergistically increased bone formation and bone volume (17), siRNA-mediated silencing of *Hivep2* in BMP-2-stimulated ST-2 cells decreased the expression and activity of ALP (Fig. 1*E*, compare *lanes 2* and *4*), whereas loss of *Hivep3* alone enhanced the osteoblast differentiation (Fig. 1*E*, compare *lanes 2* and *5*). Interestingly, combined transfection of siHivep2 with siHivep3 negated the enhancement of ALP production by *Hivep3* knockdown (Fig. 1*E*, compare *lanes 2, 5,* and *8*). Similar to siHivep2, *Hivep1* siRNA inhibited ALP activity; however, there was no synergistic or additive effect on combined knockdown of *Hivep1* and *Hivep2*. These results suggest that, in ST-2 bone marrow stromal cells, the cell autonomous actions of Hivep genes are diverse and show no cooperation in osteoblast differentiation and that Hivep1 and Hivep2 promote the counteraction of the suppressive effect of Hivep3. In contrast, in an siRNA-mediated knockdown assay in ATDC5 chondrocytes, siHivep1, siHivep2, and siHivep3 all decreased the BMP-2-induced expression of the chondrocyte-specific type XI collagen gene (*Col11a2*) (Fig. 1*F*). A similar result was observed in another chondrocytic cell line, C3H10T1/2, where knockdown of both *Hivep2* and *Hivep3* decreased the level of a chondrocyte marker, type II collagen gene (*Col2a1*) (Fig. 1*G*). In both experiments in chondrogenic cells, the combined loss of the Hivep genes showed some additive effects.

Hivep3 Suppresses Osteoblast Differentiation in Vitro—Although the mRNA level of Runx2 was comparable between wild-type and Hivep3 knock-out cells, the protein levels of Runx2, as well as the mRNA levels of the early osteoblast differentiation markers osterix (*Sp7*), alkaline phosphatase (*Alpl*), activating transcription factor 4 (*Atf4*), and bone sialoprotein (*Ibsp*) and of the late maturation marker osteocalcin (*Bglap2*) increased in knock-out osteoblasts (10). We first checked if this effect could be reproduced via siRNA-mediated knockdown in osteoblastic cell lines. We used the mouse bone marrow stromal cell line ST-2 as a model for premature osteoblast progenitors and MC3T3-E1 mouse calvaria-derived osteoblasts as mature osteoblasts. In both MC3T3-E1 and ST-2 cells, ~50% knockdown was achieved by transfection of siHivep3 (Fig. 2, *A* and *C*). As expected, *Hivep3* silencing did not have any effect on the mRNA expression of *Runx2* (Fig. 2, *A* and *C*). In ST-2 cells treated with cycloheximide to block *de novo* synthesis of Runx2

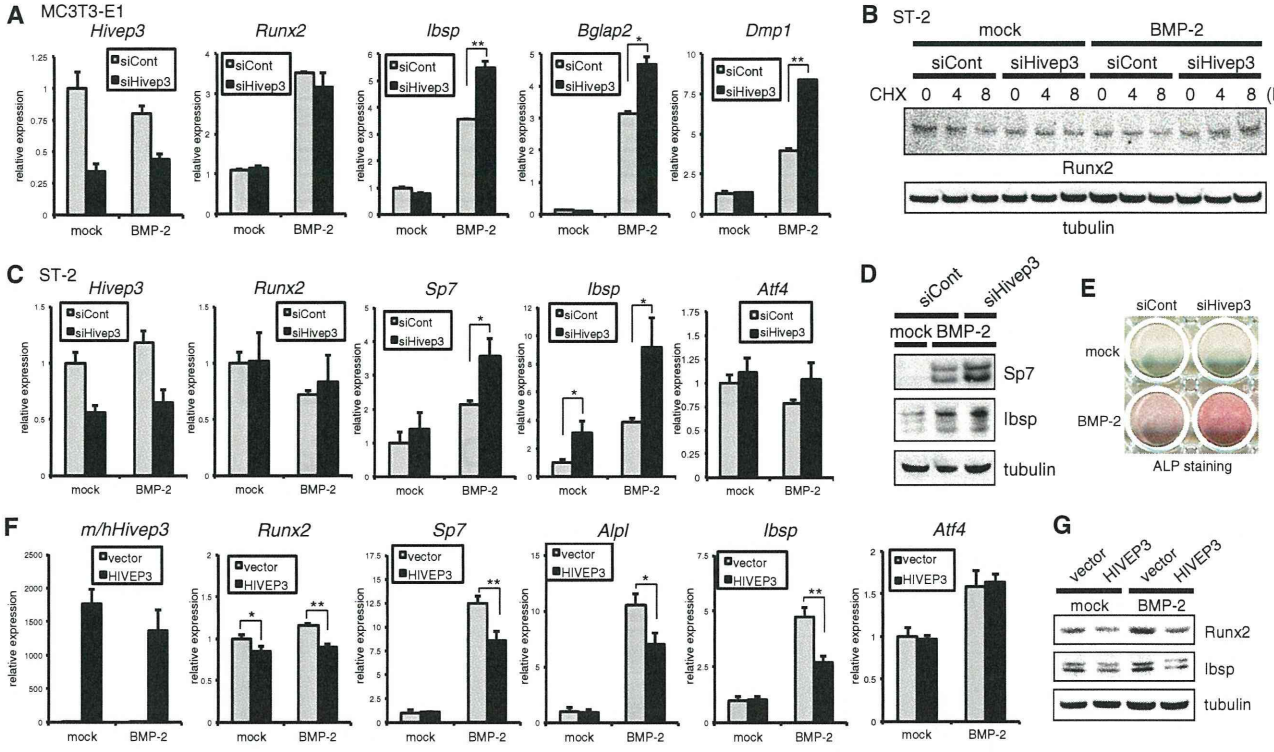

FIGURE 2. **Silencing of *Hivep3* increases protein stability of Runx2 to promote BMP-2-induced osteoblast differentiation.** *A*, MC3T3-E1 osteoblasts were transfected with siRNA for *Hivep3* with or without BMP-2 treatment (300 ng/ml) for 6 days. qRT-PCR analysis was performed for the indicated genes. *B*, siRNA-transfected ST-2 cells were treated with 100 μg/ml cycloheximide (*CHX*) with or without BMP-2 treatment (300 ng/ml) for the indicated time points. Cell lysates were analyzed by immunoblotting with an anti-Runx2 antibody. Tubulin served as a loading control. *C*, ST-2 cells were transfected with siRNA for *Hivep3* with or without BMP-2 treatment (300 ng/ml) for 3 days. The expression level of the indicated genes was examined by qRT-PCR. *D*, ST-2 cells were transfected with siRNA for *Hivep3* with BMP-2 treatment (300 ng/ml) for 7 days. Cell lysates were analyzed by immunoblotting with the indicated antibodies. Tubulin served as a loading control. *E*, ST-2 cells were transfected with *Hivep3* siRNA and stimulated with BMP-2 (300 ng/ml) for 6 days. ALP staining was performed. *F*, ST-2 cells were transfected with a human HIVEP3 expression vector and further stimulated with BMP-2 (300 ng/ml) for 4 days. The expression of the indicated genes was evaluated by qRT-PCR. *G*, ST-2 cells transfected with a human HIVEP3 expression vector were stimulated with BMP-2 (300 ng/ml) for 5 days. Cell lysates were analyzed by immunoblotting with the indicated antibodies. Tubulin served as a loading control. *, $p < 0.05$; **, $p < 0.01$.

protein, the protein level of Runx2 decreased in a time-dependent manner (Fig. 2*B*), although the protein expression was maintained in siHivep3-transfected cells. Moreover, combined induction of BMP-2 and siHivep3 in ST-2 cells increased Runx2 protein in a time-dependent fashion (Fig. 2*B*). Therefore, siRNA-mediated silencing of *Hivep3* stabilized Runx2 protein. As a result, expression of *Sp7*, *Ibsp*, and *Bglap2* was up-regulated in MC3T3-E1 and ST-2 cells (Fig. 2, *A* and *C*). In addition, the expression of an osteocyte marker, dentin matrix protein 1 (*Dmp1*), was elevated by *Hivep3* knockdown in MC3T3-E1 osteoblasts (Fig. 2*A*). The siHivep3-mediated increase of osteoblastic differentiation in ST-2 cells was confirmed by immunoblotting against Sp7 and Ibsp (Fig. 2*D*) or ALP staining (Fig. 2*E*). We introduced the human *HIVEP3* gene in ST-2 cells through transfection and confirmed the transgene expression by qRT-PCR (Fig. 2*F*). HIVEP3 suppressed BMP-2-induced osteoblast differentiation (Fig. 2, *F* and *G*) and protein expression of Runx2 (Fig. 2*G*). Interestingly, the mRNA expression of *Runx2* decreased following transfection with HIVEP3. As HIVEP3 destabilizes Runx2 protein, this result is likely due to loss of auto-induction of Runx2 (22), in which endogenous Runx2 mRNA expression increased in Runx2 transgenic mice (23). In both cases of knockdown and overexpression of *Hivep3*, expression of *Atf4* did not change (Fig. 2, *C* and *F*), although it increased in *Hivep3* knock-out osteoblasts (10).

Reduced Alg2 Gene Expression Following Knockdown of Hivep3—We next screened for genes whose expression was commonly reduced in both ST-2 cells and MC3T3-E1 cells upon *Hivep3* silencing by microarray analysis. The genes with decreased expression in MC3T3-E1 or ST-2 cells by >1.5-fold are listed in supplemental Table 5 (38 genes) or supplemental Table 4 (74 genes), respectively. Among these genes, only five were commonly down-regulated by siHivep3 in the two cell lines (Fig. 3*A*). For more stringent screening, we further increased the cutoff threshold to a >1.8-fold decrease, which left two genes each in the two cell lines, *Lypla2* and *Alg2* in MC3T3-E1 cells and *Alg2* and *Igfbp5* in ST-2 cells (Fig. 3*A*). Therefore, *Alg2* most commonly showed a decrease in expression due to *Hivep3* knockdown in both MC3T3-E1 and ST-2 cells. Asparagine-linked glycosylation (ALG) is one of the most common protein modification reactions in eukaryotic cells, as many proteins that are translocated across or integrated into the rough ER carry *N*-linked oligosaccharides (24). Alg2 is an α-1,3-mannosyltransferase forming a type I transmembrane protein on the ER, with its active site being cytosolically oriented (25). To date, no information has been reported to link

A

MC3T3-E1				
gene symbol	gene description	siCont	siHivep3	fold decrease
Lypla2	lysophospholipase 2	855.57886	385.55112	2.219106146
Alg2	**asparagine-linked glycosylation 2**	**1875.0286**	**875.0924**	**2.142663563**
Igfbp5	insulin-like growth factor binding protein 5	3540.0374	2207.5708	1.60358952
Ankfy1	ankyrin repeat and FYVE domain containing 1	1102.1857	719.4798	1.531920285
Gpr133	G protein-coupled receptor 133	545.9816	362.30106	1.50698317

ST-2				
gene symbol	gene description	siCont	siHivep3	fold decrease
Alg2	**asparagine-linked glycosylation 2**	**568.02734**	**314.0774**	**1.808558464**
Igfbp5	insulin-like growth factor binding protein 5	179.31311	99.23038	1.807038429
Lypla2	lysophospholipase 2	586.02966	349.82162	1.675224247
Ankfy1	ankyrin repeat and FYVE domain containing 1	1006.6627	650.5681	1.547359454
Gpr133	G protein-coupled receptor 133	93.81231	61.831158	1.517233593

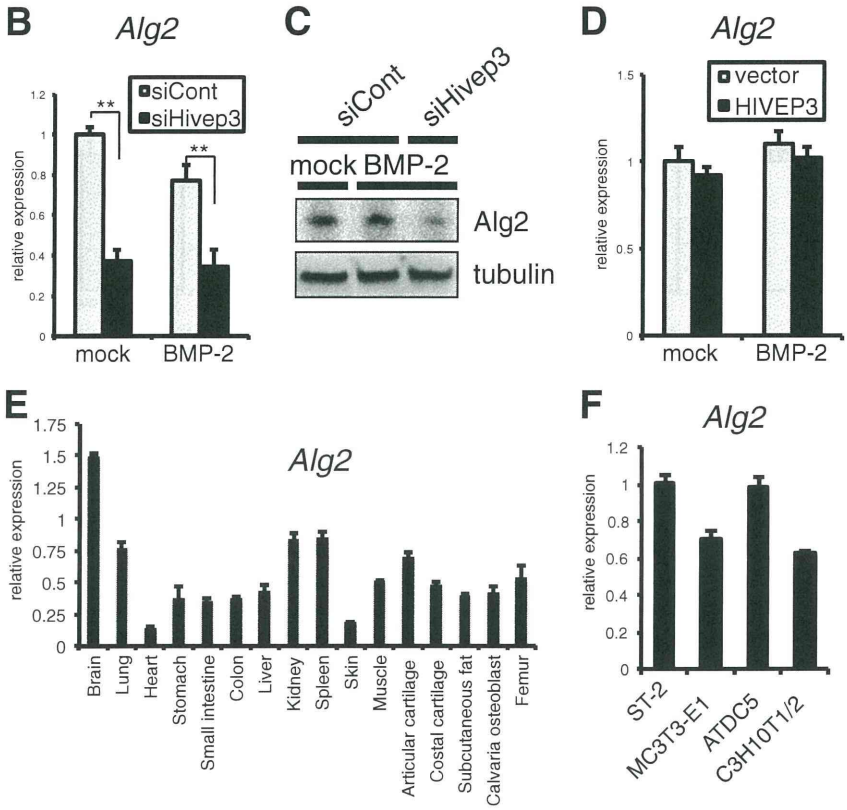

FIGURE 3. **Expression of the *Alg2* gene is reduced upon knockdown of *Hivep3* in osteoblastic cells.** *A*, siRNA for *Hivep3* was transfected into MC3T3-E1 or ST-2 cells prior to treatment with BMP-2 (300 ng/ml) for 2 days and analyzed by microarray. A list of five genes with decreased signal intensity, in common between MC3T3-E1 and ST-2 cells, is presented. *B*, ST-2 cells were transfected with siRNA for *Hivep3* with or without BMP-2 treatment (300 ng/ml) for 3 days. The expression level of *Alg2* was examined by qRT-PCR. *C*, ST-2 cells were transfected with siRNA for *Hivep3* with BMP-2 treatment (300 ng/ml) for 7 days. Cell lysates were analyzed by immunoblotting with an anti-Alg2 antibody. Tubulin served as a loading control. *D*, ST-2 cells were transfected with a human HIVEP3 expression vector to be stimulated with BMP-2 (300 ng/ml) for 4 days. The expression of *Alg2* was evaluated by qRT-PCR. *E*, tissue cDNA panel of a 3-month-old mouse was subjected to real time PCR for *Alg2*. *F*, expression level of *Alg2* in the indicated cell lines was examined by a qRT-PCR assay. **, $p < 0.01$.

Alg2 to cell differentiation. We confirmed the microarray results by qRT-PCR (Fig. 3*B*) or immunoblotting (Fig. 3*C*) and verified that knockdown of *Hivep3* in ST-2 cells decreased the level of *Alg2* by over 50%. However, forced expression of HIVEP3 did not increase *Alg2* expression (Fig. 3*D*). We next examined the tissue distribution of *Alg2* in 3-month-old mice by quantitative PCR analysis of a tissue cDNA panel (Fig. 3*E*). In tissues with low expression of *Hivep3* (Fig. 1*C*), *i.e.* the heart or skin, *Alg2* also showed a minimum level of expression, although both genes were highly expressed in the brain and lungs, suggesting a linkage between the levels of the two genes. However, there were some exceptions, *e.g. Hivep3* was expressed at high levels in fat, cartilage, and bone, whereas *Alg2* was detected at a moderate level in these tissues. From the osteoblastic and/or chondrocytic cell lines, MC3T3-E1 showed a significantly high level of *Hivep3* expression (Fig. 1*D*), whereas *Alg2* was detected in a relatively ubiquitous pattern (Fig. 3*F*). These results suggest that Hivep3 is essential but not sufficient for the expression of *Alg2*.

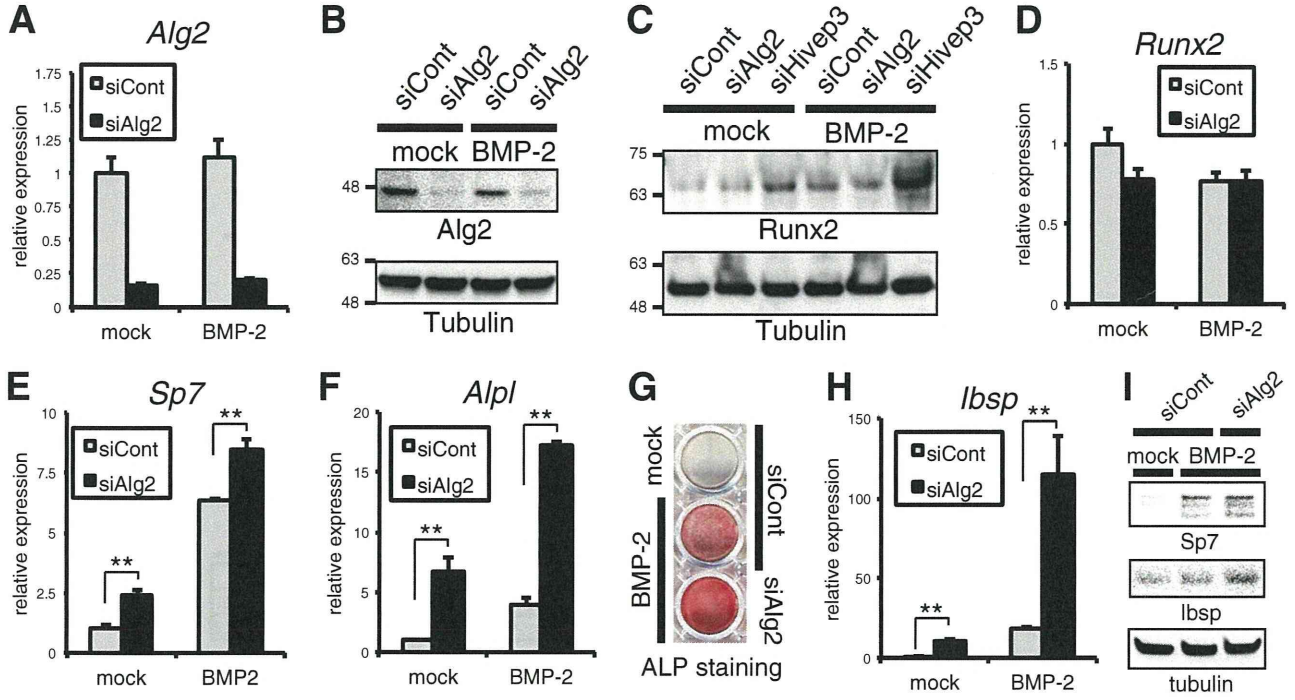

FIGURE 4. **Loss of Alg2 enhances osteoblast differentiation in ST-2 cells without affecting the protein level of Runx2.** *A* and *B*, ST-2 cells were transfected with siRNA for *Alg2* with or without BMP-2 treatment (300 ng/ml) for 3 days. Knockdown efficiency for *Alg2* was examined by qRT-PCR (*A*) or by immunoblotting (*B*). *C*, ST-2 cells were transfected with siRNA for *Alg2* or *Hivep3* with or without BMP-2 treatment (300 ng/ml) for 3 days. Cell lysates were analyzed by immunoblotting with an anti-Runx2 antibody. Tubulin served as a loading control. *D–F*, ST-2 cells were transfected with siRNA for *Alg2* with or without BMP-2 treatment (300 ng/ml) for 3 days. Expression of indicated genes was analyzed by qRT-PCR. *G*, ST-2 cells were transfected with siRNA for *Alg2* and treated with BMP-2 (300 ng/ml) for 6 days. ALP staining was performed. *H*, ST-2 cells were transfected with siRNA for *Alg2* with or without BMP-2 treatment (300 ng/ml) for 3 days. Expression of *Ibsp* was analyzed by qRT-PCR. *I*, ST-2 cells were transfected with siRNA for *Alg2* with BMP-2 treatment (300 ng/ml) for 2 days. Cell lysates were analyzed by immunoblotting with indicated antibodies. **, $p < 0.01$.

Loss of Alg2 Promotes Osteoblast Differentiation in ST-2 Cells without Affecting the Protein Level of Runx2—To investigate the possible role of Alg2 in osteoblast differentiation, siRNA for *Alg2* was transfected into ST-2 cells to obtain an ~80% decrease in mRNA expression (Fig. 4*A*) and in protein level (Fig. 4*B*). Although silencing of *Hivep3* increased the level of Runx2 protein, siAlg2 had no effect (Fig. 4*C*). As expected, loss of Alg2 also did not change the RNA level of Runx2 (Fig. 4*D*). However, *Alg2* knockdown mildly enhanced *Sp7* expression (Fig. 4, *E* and *I*), although it dramatically increased the expression (Fig. 4*F*) and activity (Fig. 4*G*) of ALP. A similar effect was seen on the level of *Ibsp* mRNA (Fig. 4*H*) and protein (Fig. 4*I*), suggesting a suppressive role of Alg2 in osteoblast maturation.

Forced Expression of Alg2 Inhibits Osteoblast Differentiation and Bone Formation—We investigated the effect of overexpression of Alg2 in osteoblasts by infection of adenovirus or lentivirus carrying an Alg2 expression cassette. In ST-2 cells, forced expression of Alg2 showed no effect on Runx2 protein level (Fig. 5*A*), whereas it strongly suppressed the expression of *Sp7*, *Alpl*, and *Ibsp* (Fig. 5*B*). The lentivirus-mediated expression of the Alg2 transgene product was confirmed at the protein and mRNA level (Fig. 5, *C* and *D*). Combined induction of *Hivep3* siRNA with the Alg2 lentivirus completely negated the enhanced expression of *Ibsp* by siHivep3, suggesting that Alg2 is a downstream mediator of Hivep3 for blocking osteoblast differentiation (Fig. 5*E*). To assess the role of Alg2 in osteoblastic bone formation, we employed the *ex vivo* culture system of calvarial bone harvested from E17.5 mouse embryo. The infection efficiency of lentivirus in bone culture was evaluated by immunofluorescence, and the V5-tagged transgene product was detected by anti-V5 antibody (Fig. 5*F*). The rate of osteoblastic intramembranous bone formation can be examined by measuring the width of the fontanelle (20). Application of BMP-2 promoted the bone formation, and it significantly decreased the fontanelle width, whereas combined induction of Alg2-expressing lentivirus cancelled the narrowing (Fig. 5*G*), indicating that Alg2 inhibited BMP-induced osteoblastic bone formation.

Alg2 Knockdown Does Not Affect ER Stress nor BMP Signaling in ST-2 Cells—A defect in ALG may affect the quality control of protein folding in the ER, which might subsequently evoke ER stress (26, 27). In addition, because physiologically mild ER stress is required for proper osteoblast differentiation and maturation (28, 29), we investigated the effect of *Alg2* siRNA on ER stress-related genes by qRT-PCR (Fig. 6*A*). Atf4, a downstream target of PKR-like endoplasmic reticulum kinase of ER stress transducer, is crucial for the expression of *Bglap2* and synthesis of type I collagen during osteoblast maturation (28, 30). *Alg2* silencing showed no remarkable effect on the *Atf4* mRNA level (Fig. 6*A*). An ER stress transducer called cAMP-responsive element-binding protein 3-like 1 (*Creb3l1*), alternatively known as Oasis, is also crucial in osteoblast differentiation (29). However, the level of *Creb3l1* was unchanged by Alg2 silencing (Fig. 6*A*). DNA damage-inducible transcript 3 (*Ddit3*), a target gene of

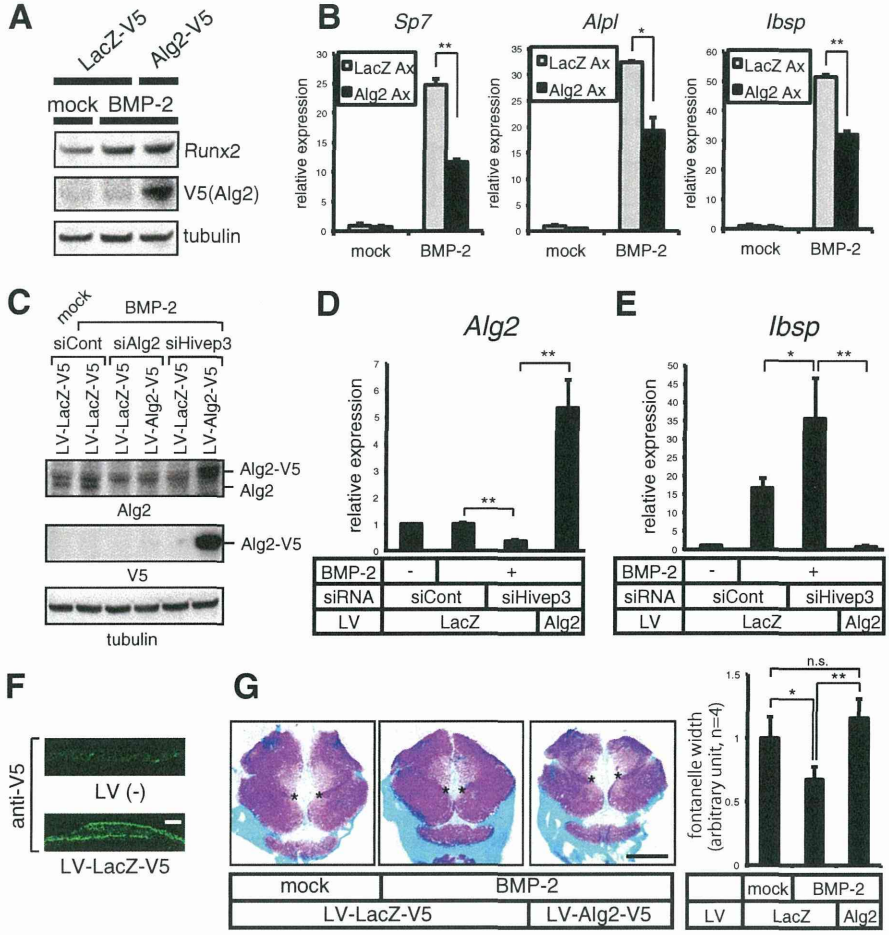

FIGURE 5. **Gain of Alg2 expression suppresses osteoblast differentiation and bone formation.** *A* and *B*, ST-2 cells were infected with V5-tagged LacZ or Alg2 adenovirus (*Ax*) and subsequently treated with BMP-2 (300 ng/ml). Cell lysates were analyzed by immunoblotting with anti-Runx2 and anti-V5 antibodies at day 6 (*A*). The expression of the indicated genes was evaluated by qRT-PCR (*B*). *C–E*, ST-2 cells were infected with LacZ or Alg2 lentivirus (*LV*). The infectants were transfected with the indicated siRNAs and stimulated with BMP-2 (300 ng/ml) for 4 days before analysis by immunoblotting with anti-Alg2 or anti-V5 antibodies (*C*). Expression of *Alg2* (*D*) or *Ibsp* (*E*) was evaluated by qRT-PCR. *F* and *G*, calvarial bones of E17.5 mouse embryos were infected with the indicated lentivirus for 16 h. Immunostaining using FITC-linked anti-V5 antibody on bone coronal sections was performed at day 2 of culture (*F*). *Scale bar*, 100 μm. LV-infected bones were treated with 300 ng/ml of BMP-2 for 3 days. Alcian blue/alizarin red staining was performed. The width of fontanelle (between *asterisks*) was measured (*G*). *Scale bar*, 2 mm. *, $p < 0.05$; **, $p < 0.01$.

Atf4 also known as CCAAT/enhancer-binding protein homologous protein (Chop), was indeed mildly up-regulated by siAlg2, but only in BMP-2-treated cells (Fig. 6*A*). The expression of a target of the Atf6 pathway, heat shock protein 5 (*Hspa5*), also known as Bip, was not altered by loss of Alg2 (Fig. 6*A*). These data suggest that ER stress is not substantially accelerated by loss of Alg2. To identify other mechanisms by which siAlg2 promotes osteoblast differentiation, we next evaluated if BMP signaling was increased by Alg2 knockdown, by assessing the expression of the representative direct target genes of the BMP-Smad pathway, *Id1* and *Smad6* (31, 32). We found no change in the level of *Id1* or *Smad6* upon Alg2 silencing (Fig. 6*B*).

Alg2 Interferes with the Transcriptional Activity and Nuclear Localization of Runx2—To test whether Alg2 interferes with Runx2 activity, we analyzed a Runx2-binding 6×OSE2 luciferase reporter. We found that Alg2 dose-dependently suppressed the Runx2-induced elevation of luciferase activity in COS-7 cells, whereas it showed no effect on the activity of 6×OSE2 reporter with Runx2-binding site mutation, suggesting that the inhibitory effect was Runx2-dependent (Fig. 6*C*). A similar result was obtained in ST-2 cells where Alg2 reduced Runx2 activity with an efficiency comparable with that of Hivep3 (Fig. 6*D*). To investigate the mechanism by which Alg2 suppresses Runx2 activity, we examined the impact of siAlg2 on the expression of an inhibitor and an activator of Runx2. Hairy/enhancer-of-split related with YRPW motif 1 (*Hey1*) is a transcriptional repressor that binds to Runx2 and suppresses its transcriptional activity (33). Contrary to our hypothesis, the expression of *Hey1* was not decreased by Alg2 knockdown; rather, it increased in a statistically significant manner (Fig. 6*E*). The expression of hairy and enhancer of split 1 (*Hes1*), which forms a complex with Runx2 to promote Runx2-dependent transcription (34, 35), was found to be unchanged by Alg2 siRNA (Fig. 6*E*). We next investigated the possibility of whether Alg2 forms a complex with Runx2 to interfere with its localization, because targeting of Runx2 to subnuclear foci, the nuclear matrix, is crucial for the bone-specific transcription of Runx2

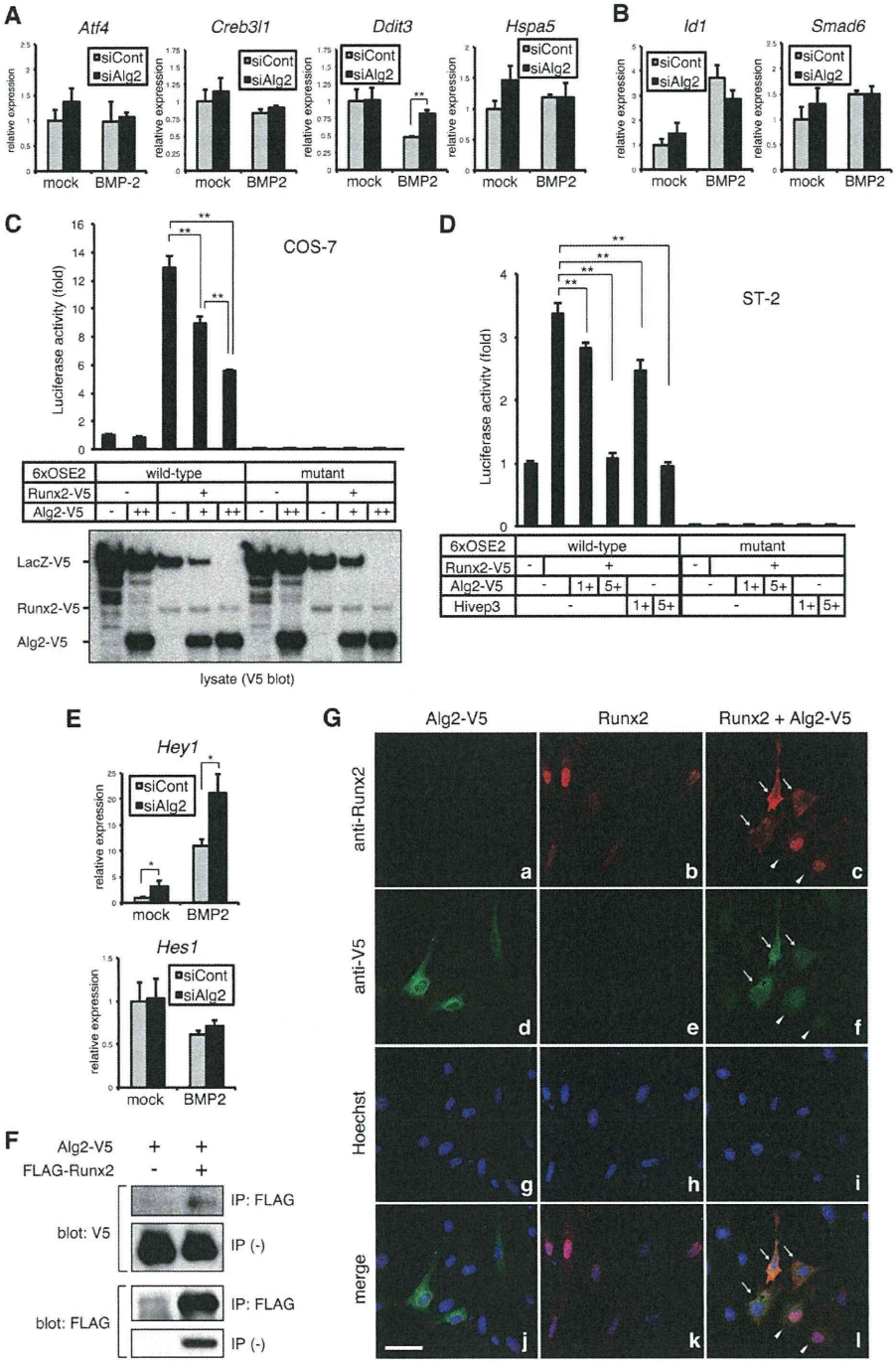

FIGURE 6. **Alg2 suppresses the transcriptional activity of Runx2.** *A* and *B*, ST-2 cells were transfected with siRNA for *Alg2* and treated with or without BMP-2 (300 ng/ml) for 3 days. Expression of indicated genes was analyzed by qRT-PCR. *C* and *D*, a luciferase reporter, 6×OSE2 luc or a Runx2-binding sequence mutant 6×OSE2 luc, and a Runx2 expression vector were transfected with or without Alg2 or Hivep3 expression plasmid into COS-7 cells (*C*) or ST-2 cells (*D*) and examined by a luciferase assay. Protein expression from the transgenes was confirmed by anti-V5 immunoblotting (*C*). *E*, ST-2 cells were transfected with siRNA for *Alg2* and treated with or without BMP-2 (300 ng/ml) for 3 days. Expression of *Hey1* and *Hes1* was analyzed by qRT-PCR. *F*, COS-7 cells were transfected with a V5-tagged Alg2 expression plasmid with or without a FLAG-tagged Runx2 vector. The cell lysate was subjected to immunoprecipitation (*IP*) with an anti-FLAG antibody and subsequent immunoblotting with an anti-V5 or anti-FLAG antibody. *G*, ST-2 cells were transfected with a V5-tagged Alg2 plasmid and/or a Runx2 expression vector. Immunofluorescence was examined with anti-Runx2 or anti-V5 antibodies. Nuclei were stained with Hoechst dye. *Scale bar*, 50 μm. *, $p < 0.05$; **, $p < 0.01$.

(36). In a co-transfection experiment using COS-7 cells, Alg2 was immunoprecipitated with Runx2 (Fig. 6*F*). By an immunofluorescence assay in ST-2 cells, we found that Alg2 protein overexpressed alone was localized to the ER (Fig. 6*G*, *panel d*), whereas Runx2 overexpressed alone was stained in the nuclei (Fig. 6*G*, *panel b*). However, in cells with combined transfection of Alg2 and Runx2, in the portion of cells in which abundant expression of Alg2 was observed, Runx2 was excluded from

nucleus and co-localized with Alg2 in the cytoplasm (*arrows*), whereas cells with a lower level of Alg2 had a nuclear pattern of Runx2 staining (*arrowheads*) (Fig. 6*G*, *panels c, f,* and *l*). These data suggest that the interaction of Runx2 with Alg2 interfered with proper subnuclear localization of Runx2, thereby decreasing its transcriptional activity.

Hivep3 Promotes the Expression of Creb3l2 and Differentiation of Chondrocytes—Next we investigated the mechanism by which Hivep3 supports chondrocyte differentiation. *Hivep3* silencing in ATDC5 chondrocytes strongly suppressed *Col2a1* in mRNA (Fig. 7*A*) and in protein levels (Fig. 7*B*). Conversely, HIVEP3 overexpression significantly enhanced expression of *Col2a1* (Fig. 7*C*). At day 21 of micromass culture, BMP-2-treated ATDC5 cells produced an abundant cartilage matrix that was stained with Alcian blue and was significantly enlarged by Hivep3 vector transfection (Fig. 7*D*). Chondrocytes secrete cartilage ECM proteins such as type II or XI collagens during differentiation, which evokes mild ER stress and induces an ER stress sensor, BBF2 human homolog on chromosome 7 (*Bbf2h7*), also known as Creb3l2. Creb3l2 plays a crucial supportive role in chondrocyte differentiation by directly inducing the expression of *Sec23a*, encoding a coat protein complex II component cargo protein responsible for the transport of secretory ECM proteins from the ER to the Golgi (18). *Atf4* expression was increased by loss of Hivep3, but only in the absence of BMP-2 (Fig. 7*E*), although gain of HIVEP3 enhanced the level in the presence of BMP-2 (Fig. 7*F*). *Ddit3* showed similar expression patterns as *Atf4*, where its basal level was elevated by siHivep3 (Fig. 7*G*), although overexpression of HIVEP3 suppressed basal expression but promoted expression in the presence of BMP-2 (Fig. 7*H*). These data indicate that the ER stress pathway of PERK-Atf4-Chop may be associated with the enhancement of BMP-2-induced differentiation by forced expression of HIVEP3. Expression of *Hspa5* was decreased or increased by knockdown or overexpression of Hivep3, respectively (Fig. 7, *I* and *J*). The expression of a spliced form of *Xbp1* was examined to monitor the inositol-requiring 1 (IRE1) pathway of ER stress and found to be suppressed or enhanced by silencing or addition of Hivep3, respectively (Fig. 7, *K* and *L*). These data suggest that Hivep3 evoked mild ER stress through the Atf6-Bip and Ire1-Xbp1 pathways. We found that *Creb3l2* expression was decreased or increased by loss or gain of Hivep3, respectively (Fig. 7, *M* and *N*). Importantly, the siHivep3-mediated reduction in *Creb3l2* expression was reflected in that of *Sec23a* (Fig. 7*O*), which may be responsible for the inhibition of differentiation.

Alg2 Is Decreased by Hivep3 Silencing in ATDC5 Chondrocytes, although Loss of Alg2 Suppresses the Expression of Creb3l2 and Chondrocyte Differentiation—We investigated whether Alg2 is a mediator of Hivep3 also in chondrocytes to affect differentiation. Indeed, knockdown of *Hivep3* strongly suppressed the expression of *Alg2* in ATDC5 chondrocytes (Fig. 8*A*). Moreover, *Alg2* siRNA inhibited the BMP-2-induced expression of type II collagen in mRNA (Fig. 8*B*) and in protein level (Fig. 8*C*). We checked whether the loss of Alg2 evoked ER stress and that the basal expression of *Atf4* (Fig. 8*D*) and *Hspa5* (Fig. 8*F*) decreased, whereas *Ddit3* expression increased in the presence of BMP-2 (Fig. 8*E*), following siAlg2 transfection. Importantly, *Creb3l2* was down-regulated by *Alg2* silencing (Fig. 8*G*), and silencing of *Alg2* or *Hivep3* both diminished the band of Creb3l2 in immunoblotting (Fig. 8*H*). Finally, we infected Alg2-expressing adenovirus in cultured mouse metatarsal cartilage, because this *ex vivo* organ culture is an excellent system to evaluate the rate of chondrocyte maturation (37). Indeed, application of BMP-2 into this cartilage culture promoted the calcification of cartilage matrix by mature hypertrophic chondrocytes (Fig. 8*J*, *1st* and *3rd lanes*). The infection efficiency of adenovirus was evaluated by immunofluorescence, and the V5-tagged transgene product was detected by anti-V5 antibody in the cartilage sample (Fig. 8*I*). Importantly, Alg2-expressing adenovirus mildly but significantly increased the zone of mature chondrocytes regardless of BMP-2 treatment (Fig. 8*J*), indicating that Alg2 promotes cartilage maturation. Taken together, these data suggest that Alg2, induced by Hivep3, is necessary for the induction of *Creb3l2* to promote chondrogenesis.

DISCUSSION

Drosophila Schnurri was one of the first partners identified for BMP-specific Smads (38, 39) for positive or negative regulation of BMP signaling. The structure of three Schnurri homologs in vertebrates, Hivep1, Hivep2, and Hivep3, is also similar to that of the fly Schnurri and shares additional features, including an unusually large size (~2500 amino acids) and acidic domains. We initially hypothesized that Hivep3 may inhibit BMP signaling to suppress osteoblast differentiation; however, the expression of the direct target genes of the BMP-Smad pathway, *Id1* or *Smad6*, was not altered by *Hivep3* knockdown in osteoblasts (data not shown). In this study, we found that the *Alg2* gene was commonly down-regulated in both ST-2 and MC3T3-E1 osteoblasts by *Hivep3* knockdown. Alg2 inhibited the activity of Runx2 without affecting its protein expression unlike Hivep3. Therefore, the Hivep3-Alg2 pathway efficiently blocks Runx2-mediated transcription and subsequent osteoblast differentiation by two approaches, regulation of protein degradation and intracellular localization. In ATDC5 chondrocytes, Alg2 expression was also controlled by Hivep3 to support chondrocyte differentiation (*Col2a1* expression), but its possible actions against Runx2 in chondrocytes remain elusive. Because Runx2 is directly crucial for transcription of the chondrocyte maturation marker gene type X collagen (*Col10a1*) in promoting chondrocyte hypertrophy (40), loss of Hivep3 or Alg2 may increase expression of *Col10a1* if they target Runx2 in chondrocytes. However, because expression of *Col10a1* arises sequentially after expression of early markers such as *Col2a1* or *Col11a2*, which had diminished expression in response to transfection with siRNA for *Hivep3* or *Alg2*, we could not clearly evaluate their effect on *Col10a1* expression (data not shown). Indeed, in *Hivep2*/*Hivep3* double knock-out mice, hypertrophic chondrocytes as well as expression of *Col10a1* have been found to decrease in the growth plates of long bones (17). Our data and those of other researchers suggest that Runx2 is not the target of Hivep3 in chondrocytes.